

## Technical Note

## Bispecific Antibody Functionalized Upconversion Nanoprobe

Hao He, Christopher B. Howard, Yinghui Chen, Shihui Wen,  
Gungun Lin, Jiajia Zhou, Kristofer James Thurecht, and Dayong Jin

*Anal. Chem.*, **Just Accepted Manuscript** • DOI: 10.1021/acs.analchem.7b05341 • Publication Date (Web): 14 Feb 2018

Downloaded from <http://pubs.acs.org> on February 17, 2018

### Just Accepted

“Just Accepted” manuscripts have been peer-reviewed and accepted for publication. They are posted online prior to technical editing, formatting for publication and author proofing. The American Chemical Society provides “Just Accepted” as a service to the research community to expedite the dissemination of scientific material as soon as possible after acceptance. “Just Accepted” manuscripts appear in full in PDF format accompanied by an HTML abstract. “Just Accepted” manuscripts have been fully peer reviewed, but should not be considered the official version of record. They are citable by the Digital Object Identifier (DOI®). “Just Accepted” is an optional service offered to authors. Therefore, the “Just Accepted” Web site may not include all articles that will be published in the journal. After a manuscript is technically edited and formatted, it will be removed from the “Just Accepted” Web site and published as an ASAP article. Note that technical editing may introduce minor changes to the manuscript text and/or graphics which could affect content, and all legal disclaimers and ethical guidelines that apply to the journal pertain. ACS cannot be held responsible for errors or consequences arising from the use of information contained in these “Just Accepted” manuscripts.



## Bispecific Antibody Functionalized Upconversion Nanoprobe

Hao He<sup>1,2</sup>, Christopher B. Howard<sup>3,4,5,\*</sup>, Yinghui Chen<sup>1,2</sup>, Shihui Wen<sup>1,2</sup>, Gungun Lin<sup>1,2</sup>, Jijia Zhou<sup>1,2</sup>, Kristofer J. Thurecht<sup>3,4,5</sup> and Dayong Jin<sup>1,2,\*</sup>

1. Institute for Biomedical Materials and Devices, School of Mathematical and Physical Sciences, Faculty of Science, University of Technology Sydney, NSW 2007, Australia

2. ARC Research Hub for Integrated Device for End-user Analysis at Low-levels (IDEAL), Faculty of Science, University of Technology Sydney, NSW 2007, Australia

3. Australian Institute for Bioengineering and Nanotechnology (AIBN), The University of Queensland, QLD 4072, Australia

4. ARC Centre for Advanced Imaging (CAI), The University of Queensland, QLD 4072, Australia

5. ARC Centre for Biopharmaceutical Innovation (CBI), The university of Queensland, QLD 4072, Australia

Corresponding authors: [dayong.jin@uts.edu.au](mailto:dayong.jin@uts.edu.au); [c.howard2@uq.edu.au](mailto:c.howard2@uq.edu.au)

### Abstract

Upconversion nanoparticles (UCNPs) are new optical probes for biological applications. To realize specific biomolecular recognition for diagnosis and imaging, the key lies in developing a stable and easy-to-use bioconjugation method for antibody modification. Current methods are not yet satisfactory regarding conjugation time, stability, and binding efficiency. Here we report a facile and high-yield approach based on a bispecific antibody (BsAb), free of chemical reaction steps. One end of the BsAb is designed to recognize methoxy polyethylene glycol (mPEG) coated UCNPs, and the other end of the BsAb is to recognize the cancer antigen biomarker. Through simple vortexing, BsAb-UCNP nanoprobe forms within 30 min and show higher (up to 54%) association to the target than the traditional UCNP nanoprobe in the ELISA-like assay. We further demonstrate its successful binding to the cancer cells with high efficiency and specificity for background-free fluorescence imaging under near-infrared excitation. This method suggests a general approach broadly suitable for functionalizing a range of nanoparticles to specifically target biomolecules.

### Introduction

Photon upconversion is an anti-Stokes process, in which sequential absorption of two or more photons results in the emission of light at a shorter wavelength than the excitation wavelength. Upconversion nanoparticles (UCNPs), one kind of luminescent nanomaterials that utilize such an anti-Stokes process, have attracted tremendous interest in recent years<sup>1,2</sup>. UCNPs can be designed to absorb near-infrared (NIR) excitation photons and emit tunable shorter-wavelength luminescence from the deep-UV to the NIR range by controlling the doped sensitizers and activators<sup>3,4</sup>. They are exceptionally photostable and low toxic,

1 making them attractive over traditional organic dyes and quantum dots as fluorescent probes for single  
2 molecule tracking<sup>5</sup>, deep-tissue optical imaging<sup>6-8</sup>, early disease diagnosis<sup>9,10</sup> and cell-targeted imaging<sup>11,12</sup>.  
3  
4 A variety of immunoassays and imaging applications rely on specific and stable binding of fluorescent  
5 nanoparticles to antibodies, which accordingly require surface functionalization of the nanoparticles with  
6 antibodies<sup>13,14</sup>. Despite the great potential of UCNPs, up to date, the facile and efficient conjugation of  
7 antibodies to UCNPs remains the critical bottleneck for its widespread applications in biological and  
8 biomedical fields<sup>15</sup>.  
9  
10

11  
12  
13 A primary reason is that UCNPs are typically synthesized in a nonpolar solvent, and they are capped with  
14 hydrophobic surfactant molecules, such as oleic acid (OA)<sup>16</sup>. At least two steps are needed to conjugate  
15 antibodies to the surface of UCNPs, including first transferring UCNPs from hydrophobic to hydrophilic,  
16 followed by conjugating hydrophilic UCNPs with antibodies<sup>15</sup>. Ligand exchange is an universal way to  
17 functionalize the surface of UCNPs with hydrophilic and active groups, such as carboxyl or amino  
18 moiety<sup>12,17</sup>. After that, carbodiimide chemistry, such as EDC method, is generally used to further conjugate  
19 antibodies to these active groups, but this approach is not only time-consuming, but it is less efficient in  
20 keeping the antibodies active and maintaining correct presentation to antigens on cell surfaces. This is  
21 because the chemical conjugation is not site-specific and often leads to blocking of the antibody binding  
22 area<sup>18</sup>.  
23  
24  
25  
26  
27  
28  
29

30  
31 Here we report for the first time bispecific antibody (BsAb) as both linker and binder for efficient  
32 conjugation of antibodies to UCNPs. BsAbs are artificial antibodies containing two different binding sites  
33 with specificity to two different targets<sup>19</sup>. In this work, we produce BsAbs through a recombinant DNA  
34 technology, for which a DNA sequence is designed to generate BsAbs with two active domains linked by a  
35 G4s linker, one domain recognizing methoxy polyethylene glycol molecules (mPEG) and the other  
36 capturing cancer cell surface antigen EphA2. This design allows direct conjugation of BsAbs with mPEG  
37 coated UCNPs in 30 min with a high bioconjugation yield, free of chemical reaction steps. We further  
38 demonstrate that BsAb conjugated UCNPs can increase the binding signal to EphA2 biomarker and enhance  
39 specific binding to prostate cancer cells, unveiling its enormous potential for cancer diagnosis and cell  
40 imaging.  
41  
42  
43  
44  
45  
46  
47  
48  
49  
50

## 51 **Experiments and materials**

### 52 **Materials**

53  
54  
55 YCl<sub>3</sub>·6H<sub>2</sub>O (99.99%), TmCl<sub>3</sub>·6H<sub>2</sub>O (99.99%), NaOH (99.9%), NH<sub>4</sub>F (99.99%), oleic acid (OA, 90%),  
56  
57  
58  
59  
60

1 1-octadecene (ODE, 90%), tetrahydrofuran (THF, anhydrous,  $\geq 99.9\%$ , inhibitor-free), hexane (anhydrous,  
2 95%), N-(3-Dimethylaminopropyl)-N'-ethylcarbodiimide hydrochloride (EDC, BioXtra),  
3 2-(N-Morpholino)ethanesulfonic acid hydrate (MES, 99.5%), H<sub>2</sub>SO<sub>4</sub> (95%), Tween 20, Ephrin type-A  
4 receptor 2 (EphA2) and anti-EphA2 antibody (IgG, produced in rabbit), are purchased from Sigma-Aldrich  
5 and used as received without further purification. Methoxy polyethylene glycol modified with phosphate  
6 group on one end (mPEG, Mw 3500) and polyethylene glycol modified with a carboxy group and a  
7 phosphate group on each end (cPEG, Mw 3500) are purchased from JenKem Technology, USA. Roswell  
8 Park Memorial Institute 1640 Medium (RPMI 1640 medium, GlutaMAX<sup>TM</sup> supplement), Fetal Bovine  
9 Serum (FBS, certified, US origin) and cell dissociation buffer (enzyme-free, PBS) are purchased from  
10 ThermoFisher.

### 19 **Synthesis of UCNPs.**

21 NaYF<sub>4</sub>: 20%Yb<sup>3+</sup>/4%Tm<sup>3+</sup> UCNPs with a size of 22 nm are prepared using our previous reported method<sup>3</sup>. 5  
22 mL of a methanol solution of RECl<sub>3</sub> (2.0 mmol, RE = Y, Yb, Tm) is magnetically mixed with 12 mL of oleic  
23 acid and 30 mL of 1-octadecene in a 100 mL three-neck round-bottom flask. The mixture is degassed under  
24 an Ar flow and heated to 150 °C for 30 min to form a clear solution and then cooled to room temperature. 15  
25 mL methanol solution containing 0.296 g of NH<sub>4</sub>F and 0.2 g of NaOH is added and stirred for 60 min. The  
26 solution is slowly heated to 150 °C and then held at this temperature for a further 30 min to completely  
27 remove methanol and some water. The reaction mixture is then quickly heated to 310 °C and aged for 1.5 h.  
28 After the solution is cooled, absolute ethanol is added to precipitate the UCNPs. After centrifuge, the  
29 precipitate is washed with cyclohexane, ethanol, and methanol four times. The washed UCNPs are  
30 redispersed in cyclohexane and stored for further experiments.

### 39 **Preparation of BsAb.**

41 The BsAb fragment consists of a single chain variable region (scFv) specific for mPEG linked to a variable  
42 region specific for EphA2, a receptor overexpressed in cancer cells. Both scFvs are linked by a glycine  
43 serine (G4s) linker. A c-myc tag is added for purification and ELISA tests. Genes encoding BsAb fragment  
44 which bind to mPEG and EphA2 are synthesized by Genart and the gene sequence is attached in SI 3.  
45 Genes are transfected into CHO cells for expression. The BsAb production and purification were performed  
46 as outlined in our previous work<sup>20</sup>.

### 52 **Preparation of mPEG coated UCNPs and cPEG coated UCNPs.**

54 To convert OA capped UCNPs to mPEG or cPEG (polyethylene glycol modified with a carboxy group)  
55 coated ones, ligand exchange method is used. 1.5 mL of 20 mg/mL UCNPs in cyclohexane are precipitated  
56

with ethanol. After centrifuge and discarding the solution, UCNPs are redispersed in 3 mL of THF with vortex and sonication. Then 1.5 mL of 200 mg mPEG or cPEG in THF solution is added. The mixed solution is stirred at room temperature for 24 h. After that, 3 mL of MiliQ water is added and mixed with shaking. Then the solution is extracted with 1 mL of hexane to remove the OA molecules. After removing the oil phase, the solution is put in vacuo overnight to evaporate organic solvents. Then the solution is dialyzed in 1 L of MiliQ water for 24 h to remove the excessive PEG molecules.

### **Bioconjugation of BsAb to mPEG-UCNPs.**

After the converting step, the mPEG-UCNPs are changed into MES buffer (pH 6.8) using a centrifuge method at a final concentration of 1 mg/mL. Then 10  $\mu$ L of mPEG-UCNPs and 10  $\mu$ L of 0.5 mg/mL of BsAb are mixed in 80  $\mu$ L of MES buffer and the solution is incubated under 37 °C with vortex for 30 min. After washing with MES buffer twice (centrifuge at 14,000 rpm for 20 min), the final settlement of conjugates is dissolved in 100  $\mu$ L of MES buffer with sonication for 5 s.

The reaction time of 30 min is determined by testing the concentration of BsAb in the conjugates under different reaction time (SI 2).

### **Optical Characterization.**

The mPEG-UCNPs and BsAb-UCNPs are separately diluted at a concentration of 10  $\mu$ g/mL in MES buffer and tested for the emission spectra using a Horiba550 spectrometer and the absorption spectra using a Nanodrop2000.

### **Indirect ELISA.**

The binding between BsAbs and mPEG-UCNPs is evaluated by indirect ELISA methods using mPEG-UCNPs immobilized on ELISA plates.

Individual wells of a 96-well plate (Nunc) are coated with 100  $\mu$ L of 50  $\mu$ g/mL of mPEG-UCNPs or without mPEG-UCNPs as negative controls overnight at room temperature. After discarding all the solution in the plate and washing each well with MEST buffer (MES + 0.05% Tween 20) three times, 400  $\mu$ L of the milk-MES buffer (MES + 2% skim milk) is added to each well and incubated for 60 min to block nonspecific binding. Then the blocking solution is discarded and 200  $\mu$ L of 50 ng/mL of BsAbs in milk-MES buffer is added to relevant wells. As control groups, 200  $\mu$ L of 50 ng/mL of control BsAbs that cannot bind to mPEG and only the buffer is also added to relevant wells, respectively. The plate is incubated at room temperature for 2 h and then washed three times with the MEST buffer. Then 100  $\mu$ L of HRP labeled anti-c-myc antibody diluted 1/5000 in milk-MES buffer is added to each well and incubated for 1 h. All the solutions are discarded and the wells are washed with the MEST buffer three times. Then 100  $\mu$ L

1 TMB solution is added to each well. After 45 s, 100  $\mu\text{L}$  of 1 M  $\text{H}_2\text{SO}_4$  is added to end the reaction. The  
2 colorimetric reactions in each well are analyzed at an absorbance of 450 nm using the plate reader. Average  
3 absorbance and standard deviation are determined for each sample.  
4

#### 5 **Dynamic Light Scanning Characterization.**

6 To determine the size of BsAbs, mPEG-UCNPs and the BsAb-UCNP nanoprobe, dynamic light scanning  
7 (DLS) test is used. For each sample, 1 mL of 50  $\mu\text{g}/\text{mL}$  sample in MES buffer is added into a cuvette and  
8 tested by Zetasizer.  
9

#### 10 **Bioconjugation of IgG Antibody to cPEG-UCNPs.**

11 After the converting step, the cPEG-UCNPs are changed into MES buffer (pH 4.5) using a centrifuge  
12 method at a final concentration of 1 mg/mL. Then 10  $\mu\text{L}$  of cPEG-UCNPs, 100  $\mu\text{g}$  of EDC and 100  $\mu\text{g}$  of  
13 NHS are mixed in 90  $\mu\text{L}$  MES buffer (pH 4.5). After 2 h gentle shaking, the sample is washed with the MES  
14 buffer twice (centrifuge at 14,000 rpm for 20 min). After the final centrifuge step, the precipitate is  
15 suspended with 50  $\mu\text{L}$  MES buffer. The solution is mixed with 50  $\mu\text{L}$  of anti-EphA2 IgG antibody (0.1  
16 mg/mL) and put into a 37  $^\circ\text{C}$  shaker overnight. After twice washing with MES buffer (centrifuge at 14,000  
17 rpm for 20 min), the sample is finally suspended in 100  $\mu\text{L}$  of MES buffer with sonication for 5 s.  
18

#### 19 **Direct ELISA-like Assay.**

20 A direct ELISA-like assay is used to compare the binding efficiency of BsAb-mPEG-UCNPs and  
21 IgG-cPEG-UCNPs to the target EphA2.  
22

23 Individual wells of a 96-well plate (Falcon) are coated with 100  $\mu\text{L}$  of EphA2 at different concentrations (0.1,  
24 1, 10 and 100 ng/mL) overnight at 4  $^\circ\text{C}$ . After discarding all the solution in the plate and washing each well  
25 with MEST buffer three times, 400  $\mu\text{L}$  of milk-MES buffer is added to each well for 60 min to block  
26 nonspecific binding. Then the blocking solution is discarded and 200  $\mu\text{L}$  of 50  $\mu\text{g}/\text{mL}$  of  
27 BsAb-mPEG-UCNPs or IgG-cPEG-UCNPs in milk-MES buffer is added. The plate is incubated at room  
28 temperature for 2 h and then washed three times with MEST buffer. The plate is dried under 60  $^\circ\text{C}$ . The  
29 signal in each well is analyzed using the emission of UCNPs by a homemade plate reader. Average signal  
30 and standard deviation are determined for each sample.  
31

#### 32 **Cancer Cell Targeted Imaging.**

33 To further broaden the application of the BsAb-UCNP nanoprobe, we test it in cell targeted imaging  
34 experiments.  
35

36 PC3 prostate cancer cells which overexpress the EphA2 and LNCaP prostate cancer cells which express  
37 undetectable levels of EphA2 are used to test the targeting of BsAb-UCNP probes.  
38

1 PC3 cells and LNCaP cells are cultured in RPMI medium with 10% FBS at 37 °C and 5% CO<sub>2</sub>. Cells are  
2 subcultured using cell dissociation buffer for cell detachment when approximately 80% confluency is  
3 reached. The cells slides are prepared one day before,  $1 \times 10^4$  cells in 2 mL cell medium are pipetted into a  
4 6-well plate with one glass cover slide in each well and incubated overnight until the cells became adherent  
5 to the cover slide. After the medium is aspirated, 500  $\mu$ L of 50  $\mu$ g/mL UCNP probes in cell medium is added  
6 to each well. As a negative control, 500  $\mu$ L of 50  $\mu$ g/mL mPEG-UCNPs in cell medium is added to PC3 cells  
7 wells. After 1 h incubation, excess particles are removed by washing with MES buffer three times. After  
8 fixed by 4% paraformaldehyde, the sample slides are sealed by vector. All the slides are imaged by an  
9 Olympus Microscopy modified with a 980 nm laser (Pigtailed DBR Single-Frequency Lasers, 1W, Thorlabs)  
10 as excitation. Average intensity and standard deviation are determined for each cell.  
11  
12  
13  
14  
15  
16  
17  
18  
19

## 20 **Results and Discussion**

### 21 **Preparation of BsAb-UCNP nanoprobe and characterization**

22 As the schematic shown in Figure 1A, we use 22 nm UCNPs with a composition of NaYF<sub>4</sub>: 20%Yb/4%Tm  
23 due to its super bright emission<sup>3</sup>. To convert UCNPs into a hydrophilic phase and modify them with mPEG  
24 molecules for BsAb conjugation, we use ligand exchange method to replace OA surfactant with mPEG onto  
25 UCNPs surface.  
26  
27  
28  
29  
30

31 The BsAb in this work is designed with two active domains linked by a G4s linker and one domain  
32 recognizes mPEG molecules with another one capturing cancer cell surface antigen EphA2. It also has a  
33 c-myc tag which is mainly used for purification and detection purposes. Although the BsAb preparation is  
34 more complicated and expensive compared with traditional IgG antibody for now, current commercial  
35 production will make it accessible to researchers as it's popular not only in the lab but also the market<sup>19</sup>.  
36  
37  
38  
39

40 The BsAb in this work consists of 517 amino acids and has a molecular weight of 55.7 kD. According to our  
41 previous work, the BsAb shows high binding affinity to both mPEG ( $K_D$  10 nM) and EphA2 ( $K_D$  1 nM)<sup>20</sup>,  
42 which is comparable to the normal EphA2 IgG antibody ( $K_D$  0.1 nM) and binders ( $K_D$  10~100 nM)<sup>21</sup>.  
43  
44  
45

46 We merely mix mPEG modified UCNPs and the designed BsAb in buffer and vortex gently for a short time  
47 and get the BsAb-UCNP nanoprobe. TEM photos in Figure 1B-D show that the morphology of UCNPs  
48 does not change after the surface modification of mPEG and BsAbs. Further emission spectra in Figure 1E  
49 show that the BsAb conjugation has no effect on optical properties of the UCNPs. And the 280 nm  
50 absorption peak (refers to protein) change in Figure 1F confirms that BsAbs bind to UCNPs.  
51  
52  
53  
54  
55  
56  
57  
58  
59  
60

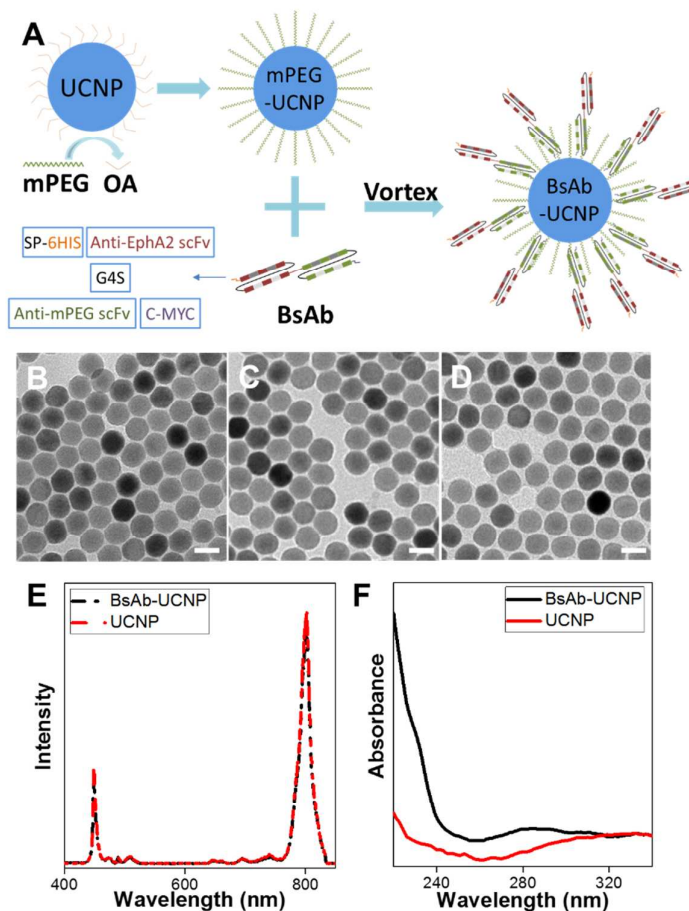


**Figure 1.** A. Scheme of the formation of BsAb-UCNP nanoprobe. And TEM pictures of UCNPs (B), mPEG-UCNPs (C), BsAb-UCNP nanoprobe (D) (Scale Bar: 20 nm). E. Emission spectra under 980 nm laser excitation of BsAb-UCNP nanoprobe and mPEG-UCNPs (at the same concentration of 10  $\mu\text{g/mL}$ ). F. Absorption spectra of BsAb-UCNP nanoprobe and mPEG-UCNPs (at the same concentration of 10  $\mu\text{g/mL}$ ).

### Validation of binding between BsAb and mPEG-UCNPs.

We use indirect ELISA to verify the successful binding of BsAb and mPEG-UCNPs (Figure 2A). The control groups include adding a BsAb that doesn't have mPEG binding ability to immobilized mPEG-UCNPs, adding second antibody alone to immobilized mPEG-UCNPs, adding BsAb to wells without mPEG-UCNPs and a blank control.

As shown in Figure 2B, the experiment group shows the significantly higher signal ( $P < 0.01$ ) than the other control groups, suggesting that the mPEG-recognizing BsAb has been successfully conjugated to mPEG-UCNPs, while neither the control BsAb nor the second antibody alone shows binding. This result indicates that the BsAb can effectively and specifically bind to mPEG-UCNPs, while mPEG-UCNPs show no binding to other proteins. Due to the high binding affinity and specificity of the BsAb, we expect mPEG-UCNPs and BsAb can self-assemble under the aqueous condition to form the BsAb-UCNP



nanoprobes.

To further prove the successful self-assembly of BsAb and mPEG-UCNPs in solution, and verify the structure of BsAb-UCNP nanoprobes (Figure 2C), we use DLS to measure the mean size of each sample. From Figure 2D, each sample shows a single peak with low Pdl value which means all samples are in well monodispersed. It shows the conjugate has a diameter of 43 nm, which indicates that BsAb has formed a single layer on top of each UCNP, because the size of BsAb is 6 nm in diameter and the mPEG-UCNPs have a diameter of 28 nm, i.e., the size of BsAb-UCNP nanoprobes is approximately the sum of one mPEG-UCNP and two BsAbs from both sides, denoting full coverage of the UCNPs with antibodies at this concentration range.

To test its stability, we use DLS to monitor the size of BsAb-UCNP nanoprobes for 8 hours after the bioconjugation and find the negligible change in size distribution (SI 1).

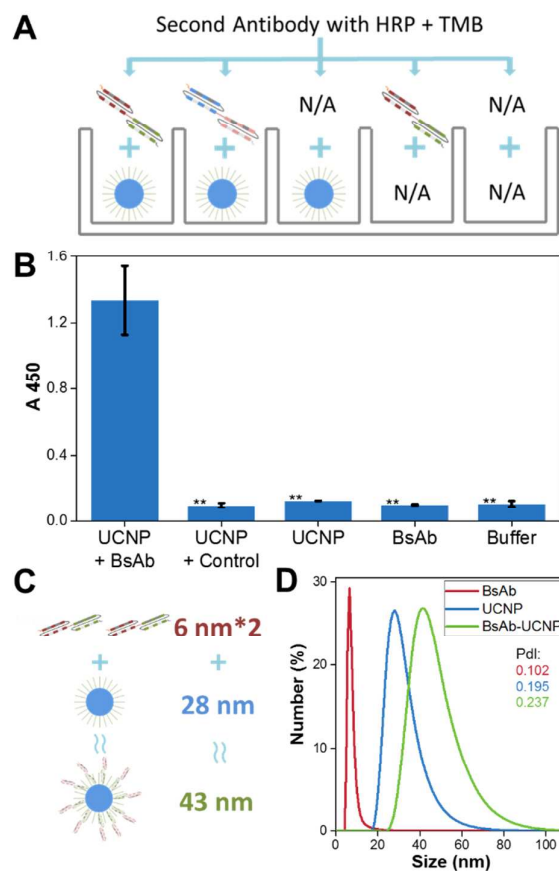


**Figure 2.** A. Scheme of the binding ELISA test. B. Results of binding ELISA tests. Each group is tested three times and error bars are shown. (Significant Difference is shown and \*\*:  $P < 0.01$ ) C. Schematic of BsAb-UCNP structure D. DLS results of BsAb, mPEG-UCNPs and BsAb-UCNP nanoprobes.

### Comparing BsAb and EDC conjugation methods

Figure 3A shows the schematic outlining of conventional EDC-coupling method that needs two

time-consuming steps, while our BsAb conjugation method is a one-step approach which is achieved with more straightforward operation and far shorter time (SI 2) under mild conditions.

Due to the drawback of the EDC method described previously, we assume that using the BsAb conjugation method will result in a higher binding efficiency. Therefore, we use a direct ELISA-like assay to compare the binding efficiency of the BsAb-UCNP nanoprobe and the IgG-UCNP nanoprobe to prostate cancer biomarker EphA2. We add these two nanoprobe separately to immobilized EphA2 at various concentrations of 0.1, 1, 10 and 100 ng/mL. From the results shown in Figure 3B, both of the nanoprobe show binding to EphA2, while the binding efficiencies of BsAb-UCNP nanoprobe are consistently higher than that of IgG-UCNP nanoprobe. The efficiency differences become more significant with the increasing of immobilized target concentration. When the immobilized target concentration is 100 ng/mL, BsAb-UCNP nanoprobe show 54% higher signal ( $P < 0.01$ ) than the IgG-UCNP nanoprobe. The results indicate that the nanoprobe developed using BsAb perform better than the nanoprobe conjugated by the traditional EDC chemical linkage method. This is because all the binding domains cannot be blocked and are shown directly to the outside by using the BsAb. Also, the BsAb has a smaller size than the normal IgG. This means that more capture molecules can be placed on the surface of the particles, which helps to increase the binding efficiency to the target.

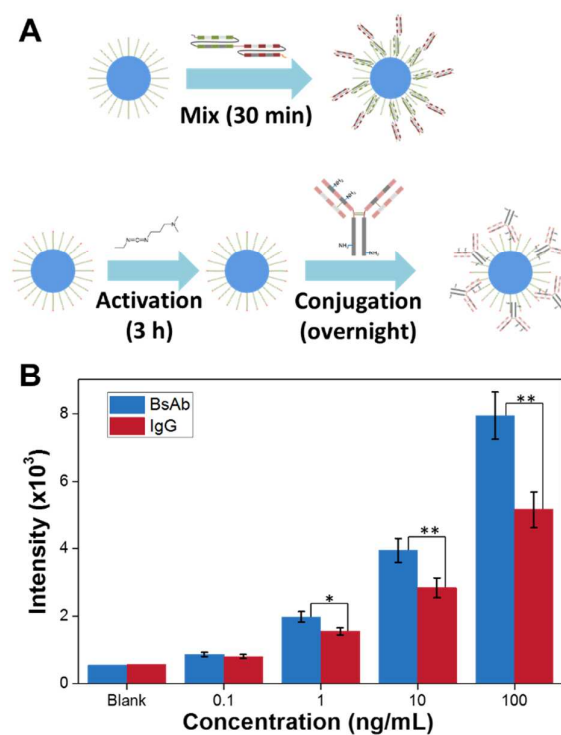


**Figure 3.** A. Scheme showing two different conjugation methods using in this study. B. Results of direct ELISA-like assay tests.

Each group is tested three times and error bars are shown. (Significant Difference is shown and \*\*:  $P < 0.01$ , \*:  $P < 0.05$ )

## Cell Imaging

After validating the higher binding efficiency of BsAb-UCNPs nanoprobe to the cancer biomarker, we further explore its use for cell imaging application, using confocal microscopy.

From the top panel of confocal images in Figure 4, overlays of fluorescence and bright-field images show that the fluorescence is mainly from the surface of the cells, confirming the accumulation of nanoprobe on the EphA2 expressed surface of PC3 cells (middle panel). In comparison, particles without BsAb show much less accumulation on PC3 cells. The effect of targeting surface receptors is also demonstrated by the negligible binding of the BsAb-UCNP nanoprobe to a cell line that only exhibits minimal expression of the EphA2 protein (LNCaP) which validates the specificity of the targeting (bottom panel). Subsequent analysis of the blue upconversion intensity per cell reveals that the experiment group shows the most intense upconversion fluorescence. All the results indicate that the BsAb-UCNP nanoprobe shows excellent performance in cell targeted imaging experiments and can be applied as an excellent bioprobe candidate for such protein biomarkers.

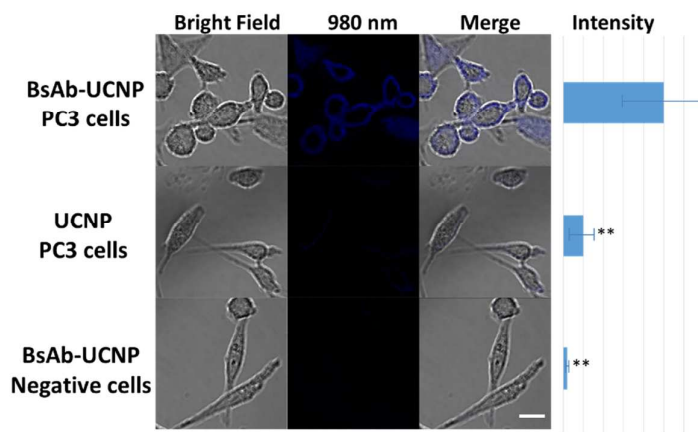


Figure 4. Confocal microscopic images of PC3 cells treated with BsAb-UCNPs, PC3 cells treated with UCNPs and LNCaP cells treated with BsAb-UCNPs. Fluorescence images (labeled with 980 nm) are obtained by collecting the blue emission in the range of 400-500 nm under the excitation of 980 nm laser. Intensity equals to the blue upconversion intensity per cell. Scale bar, 20  $\mu$ m. (Significant Difference is shown and \*\*:  $P < 0.01$ , \*:  $P < 0.05$ )

## Conclusion

In conclusion, we have developed a straightforward method for direct conjugation of UCNPs and antibodies through applying BsAb. The approach is a one-step strategy and avoids chemical reaction. And it owns a better performance in operation time and binding efficiency than the commonly used EDC conjugation

method. We subsequently demonstrated that the BsAb-UCNP nanoprobe conjugated by the developed approach could be applied in cell targeted imaging with high specific binding efficiency. This approach will promote the applicability of UCNP and can be applied to all nanomaterials with a variety of compositions, sizes and shapes and utilize a variety of antibodies for broad applications in imaging and diagnosis.

## Reference

- (1) Wang, J.; Deng, R.; Macdonald, M. A.; Chen, B.; Yuan, J.; Wang, F.; Chi, D.; Andy Hor, T. S.; Zhang, P.; Liu, G.; Han, Y.; Liu, X. *Nat. Mater.* **2014**, *13* (2), 157–162.
- (2) Zhou, B.; Shi, B.; Jin, D.; Liu, X. *Nat. Nanotechnol.* **2015**, *10* (11), 924–936.
- (3) Zhao, J.; Jin, D.; Schartner, E. P.; Lu, Y.; Liu, Y.; Zvyagin, A. V.; Zhang, L.; Dawes, J. M.; Xi, P.; Piper, J. A.; Goldys, E. M.; Monro, T. M. *Nat. Nanotechnol.* **2013**, *8*, 729.
- (4) Lu, Y.; Zhao, J.; Zhang, R.; Liu, Y.; Liu, D.; Goldys, E. M.; Yang, X.; Xi, P.; Sunna, A.; Lu, J.; Shi, Y.; Leif, R. C.; Huo, Y.; Shen, J.; Piper, J. A.; Robinson, J. P.; Jin, D. *Nat. Photonics* **2014**, *8* (1), 32–36.
- (5) Gargas, D. J.; Chan, E. M.; Ostrowski, A. D.; Aloni, S.; Altoe, M. V. P.; Barnard, E. S.; Sanii, B.; Urban, J. J.; Milliron, D. J.; Cohen, B. E.; Schuck, P. J. *Nat. Nanotechnol.* **2014**, *9* (4), 300–305.
- (6) Xiong, L.; Chen, Z.; Tian, Q.; Cao, T.; Xu, C.; Li, F. *Anal. Chem.* **2009**, *81* (21), 8687–8694.
- (7) Yao, C.; Wang, P.; Zhou, L.; Wang, R.; Li, X.; Zhao, D.; Zhang, F. *Anal. Chem.* **2014**, *86* (19), 9749–9757.
- (8) Levy, E. S.; Tajon, C. A.; Bischof, T. S.; Iafrati, J.; Fernandez-Bravo, A.; Garfield, D. J.; Chamanzar, M.; Maharbiz, M. M.; Sohal, V. S.; Schuck, P. J.; Cohen, B. E.; Chan, E. M. *ACS Nano* **2016**, *10* (9), 8423–8433.
- (9) Farka, Z.; Mickert, M. J.; Hlaváček, A.; Skládal, P.; Gorris, H. H. *Anal. Chem.* **2017**, *89* (21), 11825–11830.
- (10) He, M.; Liu, Z. *Anal. Chem.* **2013**, *85* (24), 11691–11694.
- (11) Wang, H.; Han, R. L.; Yang, L. M.; Shi, J. H.; Liu, Z. J.; Hu, Y.; Wang, Y.; Liu, S. J.; Gan, Y. *ACS Appl. Mater. Interfaces* **2016**, *8* (7), 4416–4423.
- (12) Li, L. Le; Wu, P.; Hwang, K.; Lu, Y. *J. Am. Chem. Soc.* **2013**, *135* (7), 2411–2414.
- (13) Nam, J.-M. *Science (80-. )*. **2003**, *301* (5641), 1884–1886.
- (14) Pu, K.; Shuhendler, A. J.; Jokerst, J. V; Mei, J.; Gambhir, S. S.; Bao, Z.; Rao, J. *Nat Nano* **2014**, *9* (3), 233–239.
- (15) Liu, Q.; Feng, W.; Li, F. *Coord. Chem. Rev.* **2014**, *273–274*, 100–110.

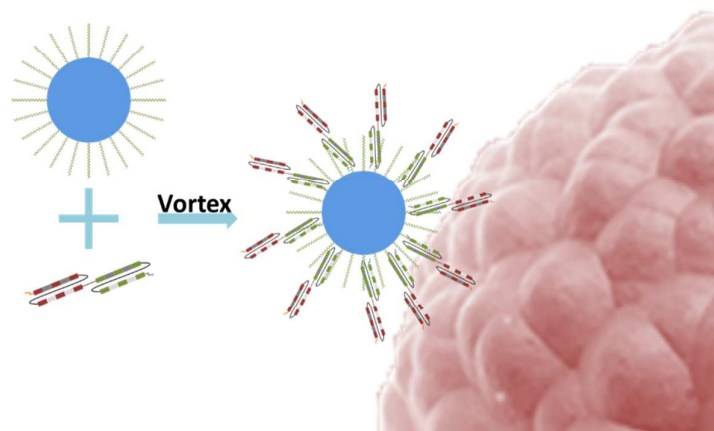
- 1 (16) Zhao, J.; Lu, Z.; Yin, Y.; McRae, C.; Piper, J. A.; Dawes, J. M.; Jin, D.; Goldys, E. M. *Nanoscale*  
2 **2013**, 5 (3), 944–952.
- 3
- 4 (17) Shi, Y.; Shi, B.; Dass, A. V. E.; Lu, Y.; Sayyadi, N.; Kautto, L.; Willows, R. D.; Chung, R.; Piper, J.;  
5 Nevalainen, H.; Walsh, B.; Jin, D.; Packer, N. H. *Sci. Rep.* **2016**, 6, 37533.
- 6
- 7 (18) Hermanson, G. T. *Bioconjugate Techniques 2nd Edition*; Academic Press, 2013.
- 8
- 9 (19) Fan, G.; Wang, Z.; Hao, M.; Li, J. *J. Hematol. Oncol.* **2015**, 8 (1), 130.
- 10
- 11 (20) Howard, C. B.; Fletcher, N.; Houston, Z. H.; Fuchs, A. V.; Boase, N. R. B.; Simpson, J. D.; Raftery, L.  
12 J.; Ruder, T.; Jones, M. L.; Bakker, C. J. De; Mahler, S. M.; Thurecht, K. J. *Adv. Healthc. Mater.* **2016**,  
13 5, 2055–2068.
- 14
- 15
- 16
- 17 (21) Ullman, C.; Mathonet, P.; Oleksy, A.; Diamandakis, A.; Tomei, L.; Demartis, A.; Nardi, C.;  
18 Sambucini, S.; Missineo, A.; Alt, K.; Hagemeyer, C. E.; Harris, M.; Hedt, A.; Weis, R.; Gehlsen, K. R.  
19 *PLoS One* **2015**, 10 (8), 1–25.
- 20
- 21
- 22
- 23

## 24 Acknowledgments

25  
26 The authors acknowledge the financial support from the China Scholarship Council (201504910696), the  
27 Australian Research Council (ARC) Future Fellowship Scheme (D.J., FF130100517), ARC Industry  
28 Transformational Research Hub Scheme (D.J., O.S., S.V., IH150100028), National Health and Medical  
29 Research Council (NHMRC) (K.J.T., APP1099321), and the Australian Research Council (K.J.T.,  
30 DP140100951). This research was conducted within the ARC Centre of Excellence in Convergent Bio-Nano  
31 Science and Technology (CE140100036). This work was performed in part at the Queensland node of the  
32 Australian National Fabrication Facility, a company established under the National Collaborative Research  
33 Infrastructure Strategy to provide nano- and micro-fabrication facilities for Australia's researchers.  
34  
35  
36  
37  
38  
39  
40  
41

## 42 TOC

43  
44  
45  
46  
47  
48  
49  
50  
51  
52  
53  
54  
55  
56  
57  
58  
59  
60



1  
2  
3  
4  
5  
6  
7  
8  
9  
10  
11  
12  
13  
14  
15  
16  
17  
18  
19  
20  
21  
22  
23  
24  
25  
26  
27  
28  
29  
30  
31  
32  
33  
34  
35  
36  
37  
38  
39  
40  
41  
42  
43  
44  
45  
46  
47  
48  
49  
50  
51  
52  
53  
54  
55  
56  
57  
58  
59  
60